Photochemical & Photobiological Sciences (2022) 21:2035–2051
https://doi.org/10.1007/s43630-022-00277-1

ORIGINAL PAPERS

Photosynthetic and ultrastructural responses of the chlorophyte *Lobosphaera* to the stress caused by a high exogenic phosphate concentration

Svetlana Vasilieva[1,2] · Elena Lobakova[1] · Olga Gorelova[1] · Olga Baulina[1] · Pavel Scherbakov[1] · Olga Chivkunova[1] · Larisa Semenova[1] · Irina Selyakh[1] · Alexandr Lukyanov[1] · Alexei Solovchenko[1,2]

Received: 13 April 2022 / Accepted: 19 July 2022 / Published online: 2 August 2022

Abstract

Biotechnology of microalgae holds promise for sustainable using of phosphorus, a finite non-renewable resource. Responses of the green microalga *Lobosphaera* sp. IPPAS C-2047 to elevated inorganic phosphate (P_i) concentrations were studied. Polyphosphate (PolyP) accumulation and ultrastructural rearrangements were followed in *Lobosphaera* using light and electron microscopy and linked to the responses of the photosynthetic apparatus probed with chlorophyll fluorescence. High tolerance of *Lobosphaera* to ≤ 50 g L^{-1} P_i was accompanied by a retention of photosynthetic activity and specific induction of non-photochemical quenching (NPQ up to 4; F_v/F_m around 0.7). Acclimation of the *Lobosphaera* to the high P_i was accompanied by expansion of the thylakoid lumen and accumulation of the carbon-rich compounds. The toxic effect of the extremely high (100 g L^{-1}) P_i inhibited the growth by ca. 60%, induced a decline in photosynthetic activity and NPQ along with contraction of the lumen, destruction of the thylakoids, and depletion of starch reserves. The *Lobosphaera* retained viability at the P_i in the range of 25–100 g L^{-1} showing moderate an increase of intracellular P content (to 4.6% cell dry weight). During the initial high P_i exposure, the vacuolar PolyP biosynthesis in *Lobosphaera* was impaired but recovered upon acclimation. Synthesis of abundant non-vacuolar PolyP inclusions was likely a manifestation of the emergency acclimation of the cells converting the P_i excess to less metabolically active PolyP. We conclude that the remarkable P_i tolerance of *Lobosphaera* IPPAS C-2047 is determined by several mechanisms including rapid conversion of the exogenic P_i into metabolically safe PolyP, the acclamatory changes in the cell population structure. Possible involvement of NPQ in the high Pi resilience of the *Lobosphaera* is discussed.

✉ Alexei Solovchenko
solovchenko@mail.bio.msu.ru

[1] Department of Bioengineering, Faculty of Biology, Lomonosov Moscow State University, Leninskiye Gory 1/12, Moscow 119234, Russia

[2] Institute of Natural Sciences, Derzhavin Tambov State University, Internatsionalnaya str. 33, Tambov 392000, Russia

Graphical abstract

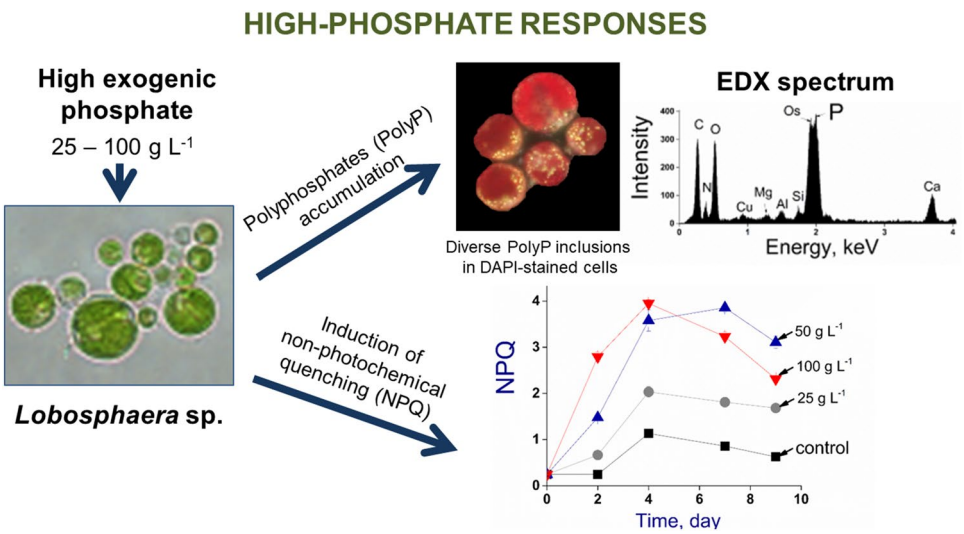

Keywords Microalgae · Stress tolerance · High exogenic phosphate · Non-photochemical quenching

1 Introduction

Phosphorus (P) is the most important component of nucleic acids, phospholipids, nucleoside phosphates including ATP other, and other important phosphometabolites crucial to the cell metabolism. The most widespread bioavailable P species in the environment is inorganic phosphate (P_i), and its internal concentration varies from 1 to 7% of cell dry weight [1, 2]. Two distinct mechanisms of P_i transport across the plasmalemma were suggested: the high-affinity system activated when the P_i concentration in the medium is low, and the low-affinity system operating when P_i is abundant [3]. In P-rich environments, microalgae (MA) exhibit two modes of P_i. The first is called overcompensation or "overshoot"; it occurs in P-starved algal cells after abrupt replenishment P_i in the medium. It is evident as a rapid, light-dependent accumulation of acid-soluble polyphosphate (PolyP). The second mode is called luxury uptake; it is displayed even by P-sufficient cells [4]. Both uptake modes result in storing of P in the cells in the amounts exceeding their momentary metabolic demand [5]. Most of the P_i taken up by the cell during luxury uptake is stored in the form of PolyP which can be later mobilized during P shortage period.

Apart from being a major P depo, PolyP are involved in a plethora of processes in the cells [6]. Thus, microorganisms deficient in the PolyP biosynthesis are characterized by abnormalities in autophagy [7], biofilm formation [8], and acclimation to both biotic and abiotic stresses, including nutrient deprivation [9]. Additionally, involvement of vacuolar PolyP in survival under osmotic or alkaline stresses was shown in microalgae [10], and it was also discovered that PolyP serves as a stabilizing scaffold for protein folding [11].

Our understanding of the mechanisms of MA acclimation and tolerance to elevated exogenic P_i levels is much more limited as compared to knowledge of P starvation effects. The question of potential P_i toxicity for MA is highly relevant to biotreatment of P-rich wastewater of diverse origin—piggery, dairy, brewery, riboflavin manufacturing, anaerobic digestion, and rubber mill effluents [5, 12]. Bioprospecting of P_i-resilient MA strains is a crucial starting point for the development of wastewater treatment biotechnologies. Testing candidate strains involves studies of the effects of a large P_i excess on their growth, photosynthesis, and PolyP accumulation in their cells. Remarkably, a "slight excess" of P_i (45 mg P L^{-1}) enhanced *Chlorella regularis* growth, while a "large excess" of P (≥ 150 mg P L^{-1}) decreased viability and caused cell damage, likely by over-accumulation of PolyP in the cells [13]. Still, the hypothesis of the PolyP involvement in the toxicity of elevated P_i to MA remains largely untested. In view of what is said above, studies of PolyP dynamics and other effects of elevated exogenic P_i would shed light on high P_i resilience of MA cells and, particularly, on the role of PolyP in these phenomena. Since photosynthesis is the primary energy source for the formation of PolyP in MA cell, linking the structural and functional responses of the photosynthetic apparatus of the cell with its acclimation to elevated exogenic P_i would be of special interest in this context. Potential role of photosynthetic apparatus in acclimation of microalgae to high-P_i toxicity remains underexplored, as well.

In the present study, we characterized the acclimation of the chlorophyte *Lobosphaera* sp. IPPAS C-2047 (referred to below as *Lobosphaera* sp.) to stress caused by elevated exogenic P_i concentrations. We attempted to link the *Lobosphaera* sp. resilience to elevated P_i levels to a large and versatile cellular P depot represented mostly by PolyP and a high physiological plasticity of its photosynthetic apparatus.

2 Materials and methods

2.1 The strain and its cultivation conditions

A chlorophyte *Lobosphaera* sp., the original strain IPPAS C-2047 deposited into the algal collection of Timiryazev Institute of Plant Physiology, Russian Academy of Sciences was used in this work. The strain was selected on the grounds of its high P_i resilience revealed during preceding screening experiments.

The preculture of the *Lobosphaera* sp. was grown at 20–23 °C in a shaker incubator (New Brunswick, Innova 44R, N.Y., USA) at 120 rpm in 0.75 L flasks with 0.3 L of P-fortified BG-11-based medium of the following composition (g L^{-1}): $NaNO_3 = 0.74$, $KNO_3 = 0.9$, $K_2HPO_4 = 0.181$, $KH_2PO_4 = 0.089$ (total $P_i = 0.160$), $MgSO_4 \cdot 7H_2O = 0.075$, $CaCl_2 \cdot 2H_2O = 0.036$, citric acid = 0.006, ferric ammonium citrate = 0.006, $Na_2EDTA \cdot 2H_2O = 0.001$, $Na_2CO_3 = 0.02$) and BG-11 trace metal solution [14] at 70 µmol PAR photons m^{-2} s^{-1} and the atmospheric CO_2 level. The culture incubated in this medium (0.160 g L^{-1} P_i) was referred to below as the control.

Growth was monitored via chlorophyll (Chl) content and dry weight (DW) measurements. DW was determined gravimetrically: 3-mL samples were vigorously mixed and filtered through pre-weighed GF/F glass fiber filters (Whatman, Maidstone, UK) and dried in a microwave oven at 100 °C to constant weight. For Chl determination, an aliquot of the cell suspension was sampled, the cells were harvested by centrifugation (3000×*g* for 5 min). Total Chl were extracted by heating the cell pellet with 2 mL of dimethyl sulfoxide (DMSO) for 10 min at 70 °C. Concentration of total Chl, Chl $a+b$ was determined in the DMSO extracts with an Agilent Cary 300 spectrophotometer (Walnut Creek, CA, USA) using previously reported equations [15].

At the beginning of each experiment, the preculture was harvested by centrifugation (700×*g* for 5 min), washed twice in the fresh medium (see above) lacking P, and resuspended in the same medium. Phosphate was added in the form of sterile potassium phosphate buffer (K_2HPO_4 and KH_2PO_4, 2:1 by mass, pH 7), the P_i concentrations of 0.32 g L^{-1}, 50 g L^{-1}, 100 g L^{-1}, and 200 g L^{-1}. The working cultures (initial Chl concentration and biomass content were 7 mg L^{-1} and 0.32 g L^{-1}, respectively) were prepared by mixing of 50 mL of the *Lobosphaera* sp. preculture cell suspension with 50 mL of the potassium phosphate buffer of each P_i concentration mentioned above. The final concentration of P_i in the media of the experimental cultures eventually used for the experiments comprised 0.16 g L^{-1} (the control, referred to below as CC), 25 g L^{-1}, 50 g L^{-1}, and 100 g L^{-1} (designated as C25, C50, and C100, respectively). The high P_i concentrations were chosen to assess the resilience of the studied *Lobosphaera* strain to the P_i levels approaching the solubility limit which can be potentially expected in the wastewater generated by rock phosphate mining and processing facilities (Solovchenko et al., in preparation). The cultures were incubated in a shaker (New Brunswick, Innova-44R, N.Y., USA) at 70 µmol PAR (photons m^{-2} s^{-1}) at 120 rpm and 20 °C for 9 days.

2.2 Estimation of intracellular phosphorus content

A slightly modified method by Ota and Kawano [16] was used for the total intracellular P determination. Briefly, cells from 15-mL aliquots of MA suspension were harvested by centrifugation (3000×*g*, 5 min) and washed 5–6 times with 50 mL of BG-11 medium lacking P. The cell pellets were disrupted in 1 mL of distilled water with G8772 glass beads (Sigma-Aldrich, USA) and 200 µl of 4% (w/v) potassium persulfate added by vigorous mixing on a V1 vortex (Biosan, Latvia) for 15 min at 4 °C and subsequent autoclaving at 121 °C for 20 min. After centrifugation of the autoclaved samples (3000×*g*, 5 min), P_i concentration was assayed in the supernatants using the molybdenum blue method [16].

2.3 Potential photosynthetic activity and photoprotection

Estimations of the potential photosynthetic activity *Lobosphaera* sp. were obtained via recording variable Chl fluorescence levels [17] using FluorCam 800 imaging PAM Chl fluorometer (PSI, Czech Republic) at days 0, 2, 5, 7, and 9 of the experiment using the built-in protocol supplied by the manufacturer. The samples were dark adapted for 15 min prior to the measurement. Maximum potential photochemical quantum yield of photosystem (PS) II was calculated as PS II $Q_y = (F_m - F_o)/F_m = F_v/F_m$, where F_o and F_m are the minimum and the maximum levels of Chl fluorescence, respectively [18]. Non-photochemical quenching (NPQ) was calculated as $NPQ = F_m/F_m' - 1$, where F_m and F_m' are dark-adapted and actinic light-adapted levels of Chl fluorescence [17].

Individual cultivation experiments were conducted to study the relationships between the changes in PS II Q_y and NPQ as a function of external P_i concentration were carried out using carbonyl cyanide

p-trifluoromethoxy-phenylhydrazone (FCCP), an uncoupler of proton gradient formation on the thylakoid membrane and photophosphorylation [18–20], and dithiothreitol (DTT), an inhibitor of the enzyme violaxanthin de-epoxidase [21, 22]. The stock solution of FCCP (Sigma-Aldrich, USA) was prepared by dissolving it in 96% ethanol. Final ethanol concentration in samples was below 1%. The equivalent amount of ethanol was added to the control cultures. The stock solution of DTT (Sigma-Aldrich, USA) prepared by dissolving it in distilled water. The stock solutions were simultaneously added to the culture 1 h after the inoculation to the final concentration of 20 nM and 2 mM for FCCP and DTT, respectively.

Our preliminary tests demonstrated that the effects of DTT and FCCP became evident already after 30-min incubation and remained stable at least for 3 days under our experimental conditions (Sect. 2.1). Since a pronounced effect of the elevated P_i levels on PS II Q_y and NPQ of the microalgae cells was already observed on the 2nd day of the experiment (see below), the cultures were incubated of the cultures with DTT and FCCP for 2 days to avoid potential side-effects of the added chemicals.

2.4 Electron microscopy

The samples of microalgae cells for transmission electron microscopy (TEM) were prepared as previously described [24]. The samples for nanoscale element analysis using energy-dispersive X-ray spectroscopy (EDX) were fixed, dehydrated, and embedded as formerly described [25]. Briefly, semi-thin sections were made with an LKB-8800 (LKB, Sweden) ultratome and examined under JEM-2100 (JEOL, Japan) microscope equipped with an LaB_6 gun at the accelerating voltage 200 kV. Point EDX spectra were recorded using JEOL bright-field scanning TEM module and X-Max X-ray detector system with ultrathin window capable of analysis of light elements starting from boron (Oxford Instruments, UK). The energy range of recorded spectra was 0–10 keV with a resolution of 10 eV per channel. At least 50 cell sections per specimen were analyzed. Spectra were recorded from different types of electron-dense inclusions (at least 30 measurements for each type of inclusions, see below). Spectra were processed with INKA software (Oxford instruments, UK) and presented in a range 0.1–4 keV.

2.5 Brightfield and fluorescence microscopy

The cells were examined under Leica DM2500 microscope equipped with a digital camera DFC 7000T of the same manufacturer. For visualization of PolyP, the cells were stained with a fluorescent dye DAPI (4′,6-diamidino-2-phenylindole) dissolved in DMSO [26]. The cells diameter was measured on the micrographs using ImageJ software (NIH, Bethesda, MA, USA). Young and mature sporangia, dead cells, oleosomes, and starch grains were counted on the bright-field and electronic micrographs. Significance of the differences between the average values at the level $p < 0.05$ was tested by Student's two-tailed *t* test using Origin software (OriginLab, Northampton MA, USA). Vegetative cells > 10 μm in diameter were considered as mature cells. The cells < 10 in diameter, including autospores, aplanospores, or zoospores, released from the sporangia were considered young cells. The proportions of mature or young cells, sporangia, and dead cells were calculated as percentages of the total cell number. The proportions of cells harboring the DAPI-stained PolyP inclusions were calculated as the percentages of the total cell number. The proportion of live and dead cells was estimated basing on the presence of the red Chl autofluorescence (in live cells) or blue fluorescence of cell walls only typical for dead cells [27].

2.6 Statistical treatment

Two independent experiments with two biological replications each ($n = 4$) were carried out. For each biological replication, three analytical replications were completed if not stated otherwise. In figures, average values together with standard deviations are presented. The significance of differences was tested using ANOVA from the analysis toolpack of the Microsoft Excel spreadsheet software.

3 Results

To assess the tolerance the *Lobosphaera* sp. to stress caused by several elevated exogenic P_i concentrations and to gain insights into the mechanisms of its acclimation to this stress, we studied growth of its cultures, structure, and function of the photosynthetic apparatus, as well as cell morphology and ultrastructure. We compared the cases of acclimation to and the toxic effects of the high P_i concentration on the *Lobosphaera* sp. cells. Special attention was paid to the dynamics of PolyP accumulation and its subcellular distribution.

3.1 The inhibition of growth and chlorophyll accumulation

Since in *Lobosphaera* sp., the daughter cells remain in aggregates after division of the mother cell, it is hard to estimate the culture growth via cell direct count. Therefore, the changes in the accumulation of biomass (via DW; Fig. 1a) and volumetric Chl content (Fig. 1b) were monitored. During 7 days of the experiment, the P_i levels up

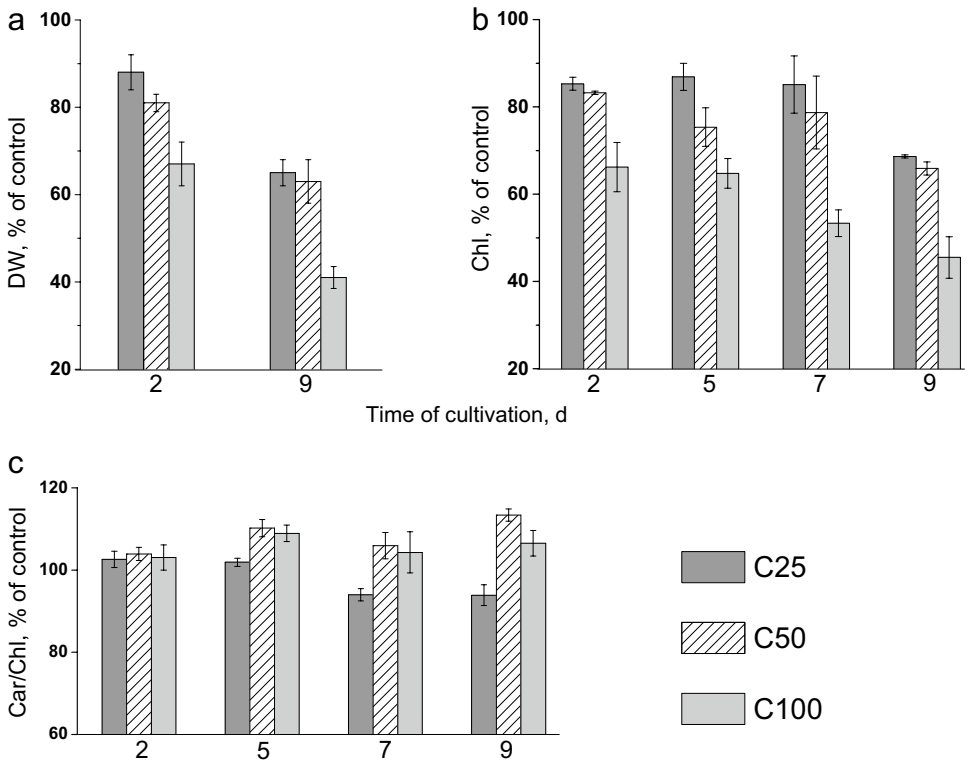

Fig. 1 The changes in **a** biomass accumulation, **b** chlorophyll accumulation, and **c** carotenoids/chlorophyll ratio in the *Lobosphaera* sp. IPPAS C-2047 cells cultivated at elevated levels of P_i (indicated on the graphs). Data are presented as means ± SD

to 50 g L^{-1} exerted a moderate inhibitory effect on the DW and Chl accumulation by the *Lobosphaera* sp. culture. Only at the 9th day, a considerable decrease in DW (37%) and Chl content (34%) was noticed. The cultures incubated in the presence of 100 g L^{-1} P_i (referred to below as "C100") showed a more pronounced decline in DW and Chl starting from the beginning of the incubation: DW declined by 59% and Chl declined by 54% relative to the control by the end of the experiment. The total Carotenoid-to-Chl ratio remaining nearly stable in the control culture (designated as "CC"), while in the C50 (50 g L^{-1} P_i) and C100 cultures, this ratio increased slightly (Fig. 1c).

3.2 Cell morphology

The *Lobosphaera* sp. incubated in the P_i-fortified BG-11 medium displayed a considerable degree of cell heterogeneity as a function of the external P_i concentration. During 9 days of the experiment, the young and mature vegetative cells, as well as the three cell types associated with culture proliferation (autosporangia, zoosporangia, and aplanosporangia) were frequently found in the studied *Lobosphaera* sp. culture (Figs. 2, 3). Zoo- and aplanosporangia dominated the CC culture, while autosporangia comprised 5–10% of all types of sporangia detected in this culture. Under the elevated P_i conditions (the experimental variants C25, C50, C100), the number of zoosporangia decreased considerably after a 5-day incubation. At the end of the experiment, zoosporangia disappeared, and the cultures were dominated by aplanosporangia. Cells with signs of plasmolysis and cell debris were also observed in the C50 (Figs. 2m, u, SI1a) or C100 cultures (Figs. 2w, SI1b-d) after 5 d incubation.

The 9-day incubation of *Lobosphaera* sp. in the presence of the elevated P_i levels did not alter the average size of young or mature cells or sporangia as compared to the control (Fig. SI2). Only at the 7th day of experiment, average size of young cells in the C25 or C50 cultures increased ($p < 0.01$; cell diameter of 7.7 ± 1.4 vs. 6.8 ± 1.7 µm, respectively; Figs. SI2c). By contrast, in the CC and C100 cultures, the diameter of young cells remained unchanged throughout the experiment ($p < 0.01$; diameter 4.9 ± 1.33 vs. 4.9 ± 1.47 µm, respectively; Fig. SI2).

3.3 The evolution of the cell population structure and polyphosphates' accumulation

At the 2nd day of the experiment, the largest percentage of young cells was noticed in the control (82%) and the smallest (46%) was in the C100 culture, while in the C25 or C50 cultures, the proportion of young cells comprised 54% and 66%, respectively (Fig. 4a). Notably, the ratio "young/mature/sporangia/dead cells" was almost constant in the CC culture throughout the experiment with domination of young cells. The highest proportion of dead cells (25%) was detected in

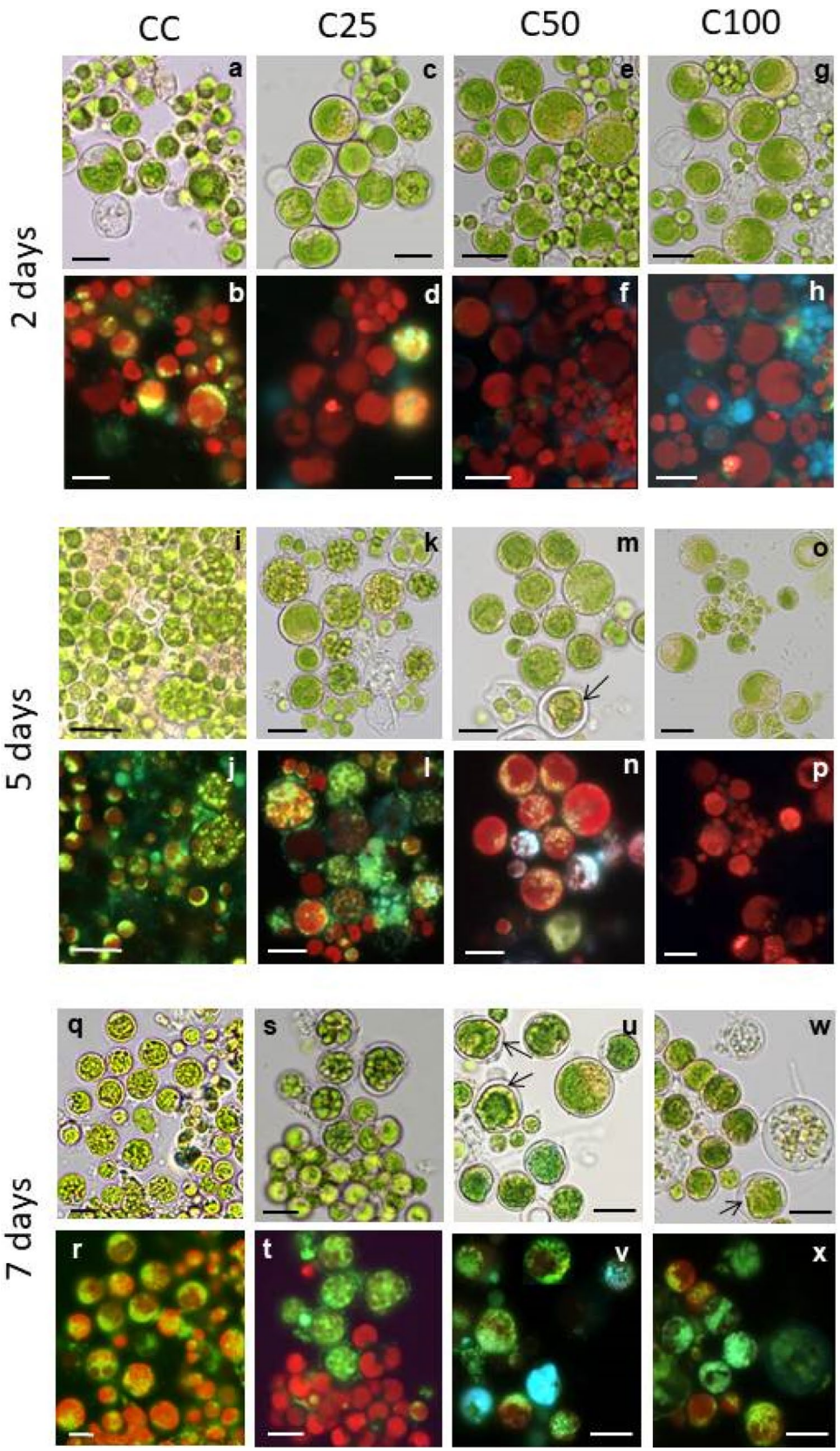

Fig. 2 Brightfield (the lines a…g, i…o, and q…w) and fluorescence (the lines b…h, j…p, and r…x) microscopy images of *Lobosphaera* sp. IPPAS C-2047 cultivated in the presence of different P_i levels (indicated at the top of columns in g L^{-1} P_i) for 2, 5, or 7th days (indicated at the left). Arrows indicate the cells with the signs of plasmolysis. Yellow–green fluorescence corresponds to the vacuolar PolyP inclusions stained with DAPI, red autofluorescence is emitted by chlorophyll, and the blue fluorescence is emitted by dead cells. Scale bar = 10 µm

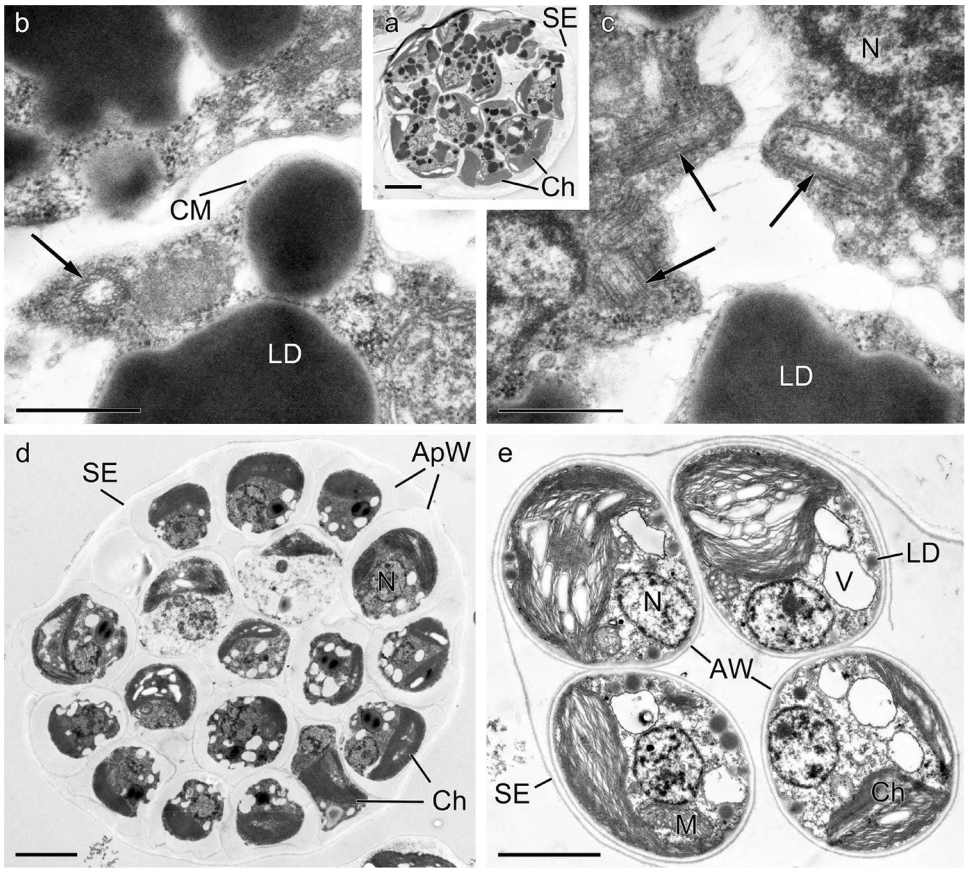

Fig. 3 Ultrastructure of the *Lobosphaera* sp. IPPAS C-2047 sporangia in modified BG-11 medium with 0.160 g $P_i L^{-1}$: **a**–**c** zoosporangium: a survey image (**a**), fragments of enlarged transverse (**b**), and longitudinal sections (**c**) of the basal area of flagella; **d** aplanosporangium, that develops from zoosporangium; **e** autosporangium. *AW* wall of autospora, *ApW* wall of aplanospora, *Ch* chloroplast, *CM* cytoplasmic membrane, *LD* lipid droplet, *N* nucleus; *M* mitochondrion, *SE* sporangium envelope, *V* vacuole. Arrows indicate basal sections of flagella. Scale bars = 2 (**a**, **d**, **e**) and 0.5 µm (**b**, **c**)

the C100 culture (Fig. 4). The highest percentage of sporangia was noticed in the C25 culture: at the 7th day of the experiment, it was 39%, while in the CC, C50, and C100 cultures, the percentage of sporangia was only 5–9% (Fig. 4c). After 9 day of incubation, young cell percentage in the C25, C50, and C100 cultures was 1.7–2.2-fold lower than that in the CC (41–52%). The highest share of sporangia was observed in C25, while in the C50 and C100 cultures, the sporangia were almost absent (Fig. 4d).

The intracellular reserves of PolyP are readily visualized by staining with DAPI; their complex with the stain yields a characteristic yellow–green fluorescence (Fig. 2). On the 2nd day of the experiment, PolyP were detected in 22% of sporangia, 19% of young cells, and in 44% of mature cells of the control culture (Figs. 2b, 4a). At the same time, PolyP were visualized only in 25% of sporangia found in the C25 cultures, whereas in the young and mature cells, PolyP were not observed at all (Figs. 2d, 4a). Although one might expect increased abundance of PolyP inclusions in the cells incubated with a high external P_i, we did not find them in the C50 or C100 cultures in the beginning of the experiment (Figs. 2f, h, 4a). Since the biosynthesis of PolyP requires a lot of energy and hence active metabolism, it is possible to think that the delay in the formation in the C50 and C100 might stem from the inhibitory effect of the high P_i concentrations on the cells which was also evidenced by a decline in culture growth (Fig. 1a).

A considerable increase in PolyP inclusions was noticed on the 5th day of the experiment: up to 95% of the control cells contained PolyP (Figs. 2j, 4b). The number of sporangia with PolyP also increased in the C25 culture (15% of mature and 34% of young cells; Figs. 2l, 4b). Remarkably, the C100 cultures lacked visible PolyP inclusions (Figs. 2p, 4b), while in the C50 cultures, PolyP appeared only at the 5th day of incubation (in 18% of mature and 62% young cells; Figs. 2n, 4b). At the 7th day of the experiment, the PolyP inclusions appeared in the C100 culture (Figs. 2x, 4c), after a certain acclimation to the high external P_i.

3.4 Total phosphorus content of the cells

The CC cells of *Lobosphaera* sp. possessed approximately constant cell P content (1.52–1.90% DW) throughout the experiment (Table 1). Even at extremely high external P_i concentration in the medium, the cell P content increased only 1.5–5.0 times in comparison with the control; the maximal level of intracellular P (9.1%) was recorded in the C100 culture incubated for 2 day (Table 1). Later, the cell P content declined in this culture. In the C25 and C50 cultures,

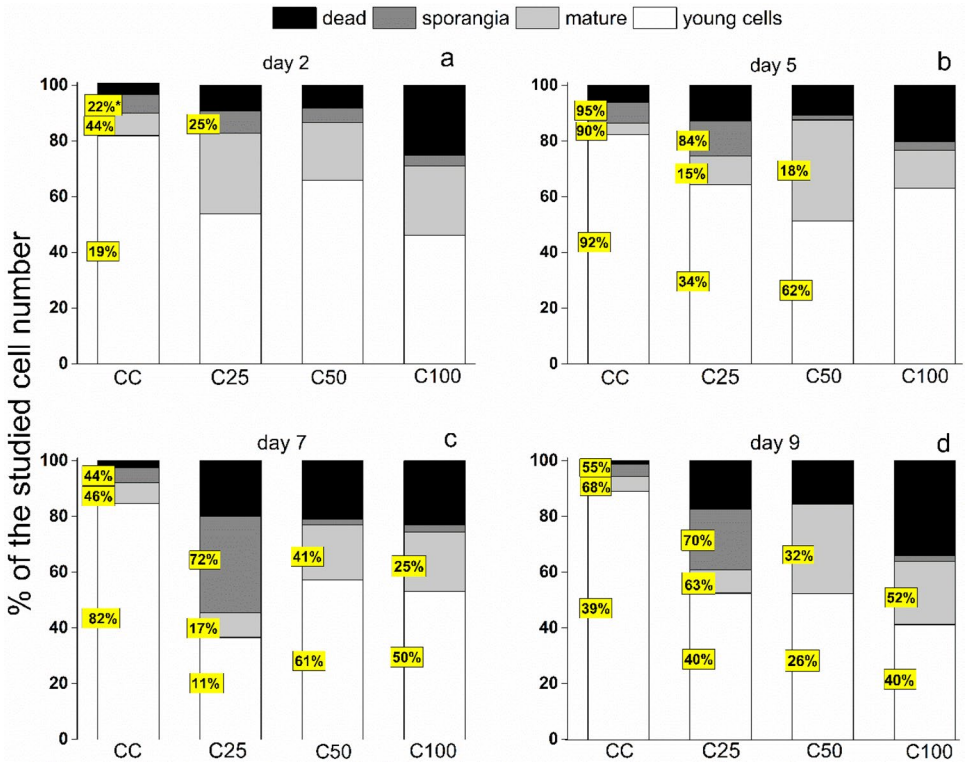

Fig. 4 The changes of the different cell type percentages and PolyP abundance in *Lobosphaera* sp. IPPAS C-2047 incubated for **a** 2, **b** 5, **c** 7, and **d** 9 days at elevated P_i level (specified at the graphs). The numbers in the yellow boxes indicate the proportion of cells harboring the DAPI-stained PolyP of the total number of cells belonging to the corresponding type (see legend at the top). Data are presented as means (see Sect. 2)

Table 1 The P percentages in DW of *Lobosphaera* sp. IPPAS C-2047 cells incubated at elevated P_i levels

Experimental variant	Incubation time			
	0 day	2 days	7 days	9 days
CC	1.52 ± 0.4[a]	1.7 ± 0.1	1.3 ± 0.1	1.9 ± 0.2
C25	1.52 ± 0.4	3.0 ± 0.5	1.9 ± 0.2	3.4 ± 0,2
C50	1.52 ± 0.4	3.7 ± 0.6	1.8 ± 0.2	4.6 ± 0.1
C100	1.52 ± 0.4	9.1 ± 0.5	2.7 ± 0.1	1.9 ± 0.3

[a]Data are presented as means ± SD

the cell P content fluctuated in the range 1.8–4.6% through the rest of the observation period.

3.5 Photosynthetic activity

The magnitude of the high-P_i stress effect on the photosynthetic activity of *Lobosphaera* sp. was estimated using the fast Chl fluorescence transients (Fig. 5, Sect. 2). The changes of the potential maximal photochemical quantum yield of photosystem II (PS II Q_y) demonstrated different trends depending on the external P_i level (Fig. 5a). The CC culture as well as the C25 and C50 cultures showed a high PS II Q_y in the range of 0.6–0.7 throughout the experiment. Only the C100 culture showed a steady decrease in PS II Q_y to 40% of the corresponding value recorded in the CC culture (triangles in Fig. 5a).

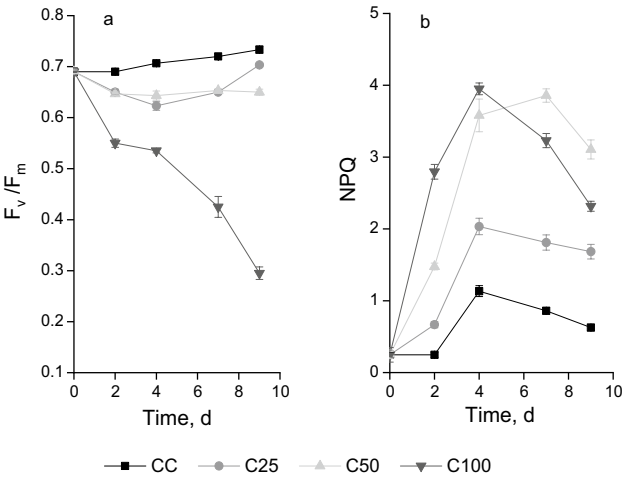

Fig. 5 Changes in **a** potential maximal quantum yield of photosystem II (F_v/F_m) and **b** non-photochemical quenching of Chl fluorescence (NPQ) in *Lobosphaera* sp. IPPAS C-2047 cells cultivated with 0.16 (control), 25, 50, and 100 g L^{-1} P_i. Data are presented as means ± SD

To assess the engagement of the photoprotective mechanisms related to dissipation of the excessively absorbed light energy in the *Lobosphaera* sp., we followed the changes in non-photochemical quenching of Chl fluorescence (NPQ) (Fig. 5b). A low level of initial NPQ (0.4–1.1) along with a high F_v/F_m (0.7–0.74) in the CC culture suggested the efficient photochemical utilization of the absorbed light energy

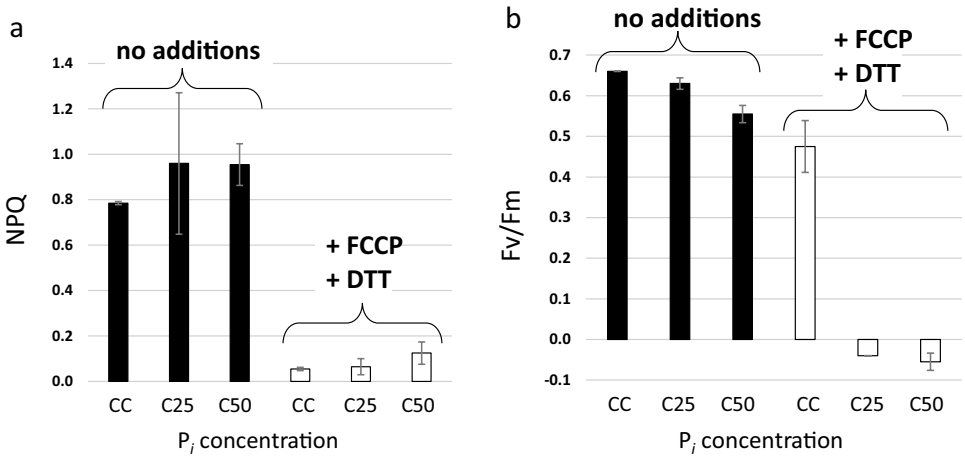

Fig. 6 Effect of chemicals blocking the formation of proton gradient on chloroplast membrane (FCCP) and a violaxanthin de-epoxidase inhibitor (DTT) on **a** non-photochemical quenching of Chl fluorescence (NPQ) and **b** potential maximal quantum yield of photosystem II (F_v/F_m) in *Lobosphaera* sp. IPPAS C-2047 cells cultivated with 0.16 (control), 25, and 50 g L^{-1} P_i. Data are presented as means ± SD (for further details, see Sect. 2)

by the microalgae under those conditions. An increase of NPQ was recorded in this culture followed by its decline. Similar trend but with much higher magnitude of NPQ increase (up to 4 in the case of the C100 culture) was displayed by the cultures incubated at the elevated P_i levels. Notably, a decline in NPQ showed by this culture was not accompanied by an increase in F_v/F_m suggesting the decline in the efficiency of the energy-dependent NPQ-based photoprotective mechanisms. At the same time, the C25 and C50 cultures possessed high F_v/F_m on the background of moderately high NPQ (Fig. 5b). A decline of NPQ on the background of F_v/F_m retention in those cases might be indicative of efficient acclimation of the cell to the elevated P_i level manifested by a high photosynthetic activity and a gradual disengagement the NPQ-related protective mechanisms in these cultures.

To better understand relationships between the retention of PS II Q_y and the increase in NPQ observed in the presence of elevated P_i concentrations, we tested the effects of FCCP, an uncoupler of photophosphorylation and proton gradient formation on the thylakoid membrane, in combination with DTT, an inhibitor of the violaxanthin de-epoxidase enzyme responsible for up-regulation of the violaxanthin cycle (Fig. 6); these compounds are collectively referred to below as "NPQ blockers". These experiments included the variants characterized by relatively high F_v/F_m (C25 and C50) together with the control (CC). The cells treated with the NPQ blockers demonstrated a low NPQ level (< 0.2), whereas in the untreated cells, NPQ was relatively high (> 0.8; Figs. 5b and 6a). At the same time, the cells treated with the NPQ blockers showed a nearly zero PS II Q_y in the presence of elevated P_i levels (C25 and C50 in Fig. 6b). Notably, at the low P_i concentration (CC; Fig. 6b), PS II Q_y was relatively high (around 0.45) and close to the values typical of the untreated cells (0.55–0.65), indicating that the added chemicals exerted only a little toxic effect per se. Overall, the results of these experiments support the existence of a relationship between the retention of a high potential photosynthetic activity and high NPQ levels registered in the presence of moderately elevated P_i concentrations.

3.6 Ultrastructural responses to elevated external orthophosphate levels

Under our experimental conditions, the CC cells retained the ultrastructure typical of the *Lobosphaera* sp. vegetative cells and closely related strains (Fig. 7a) [26, 28–30]. Most vegetative cells featured a single cup-shaped chloroplast with a large central pyrenoid traversed by several parallel thylakoids (Fig. 7a). Heterogeneity of the structure and condition of the thylakoids was observed. In most of the spores residing in the sporangia (Fig. 3) and those of the young cells, their chloroplast thylakoids featured a contracted lumen throughout the experiment. The tightly packed granal thylakoids dominated on the periphery of the chloroplasts. Their lumen was the narrowest (4–5 nm) on the 2nd day of incubation; Fig. 7b) on the 9th day the lumen was 5–10 nm wide. The thylakoid lumen of the chloroplast of mature vegetative cells was expanded (44–190 nm, mostly in the central part of the chloroplast; Figs. 7a, b).

A general ultrastructural feature of *Lobosphaera* sp. incubated for 2 days in the presence of the elevated P_i was comprised by expanded thylakoid lumen observed both on the peripheral and the central part of the chloroplast (Figs. 8a, d, e; SI3a; SI4). Moreover, some cells of the *Lobosphaera* sp. incubated at an elevated P_i level displayed the unstacking of granal thylakoid membrane (Fig. 8d). It should be noted that most of the vegetative cells incubated at 50 g L^{-1} or at a lower P_i level retained the expanded thylakoid up to the 9th day of the experiment (Fig. SI3e, f). By contrast, the C100 cells displayed a contracted thylakoid lumen and the signs of membrane destruction, e.g., fragmentation of the thylakoids (Fig. 8g).

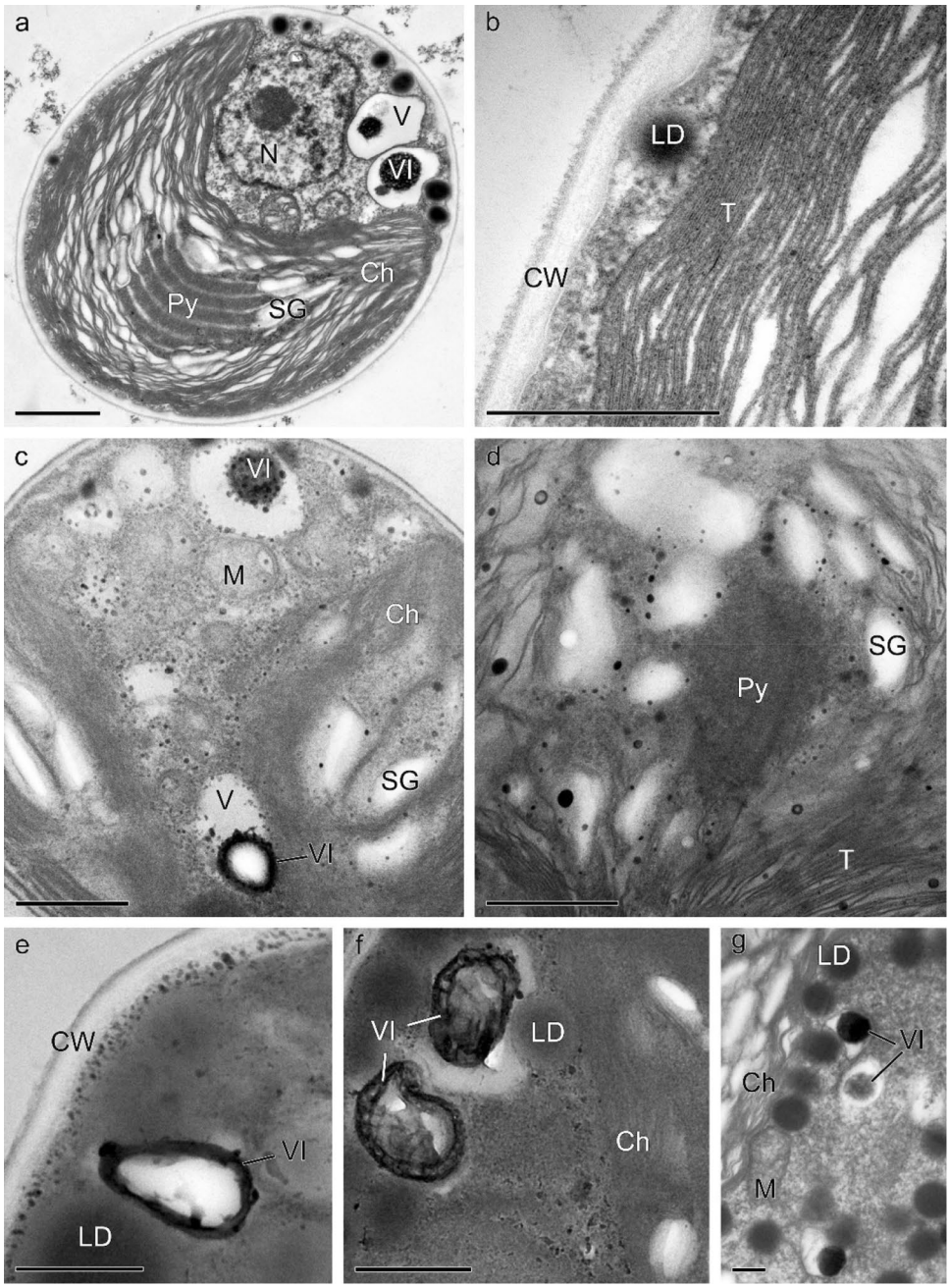

Fig. 7 Ultrastructure of the *Lobosphaera* sp. IPPAS C-2047 cells in CC (**a**, **b**), C25 (**c**, **d**), C100 (**e**, **f**), and C50 (**g**) cultures. TEM images of the ultrathin (**a**, **b**) or semi-thin sections (**c**–**g**) are presented including a survey image of the cell (**a**) and its chloroplast (**b**, enlarged); vacuoles with assorted granules (**a**, **c**, **e**–**g**); spherules in the cytoplasm (**c**), thylakoid lumen and stroma of the chloroplast (**d**), vacuoles (**c**), cell wall (**e**); the small particles of irregular shape in the cytoplasm (**f**). *Ch* chloroplast, *CW* cell wall, *LD* lipid droplet, *N* nucleus, *M* mitochondrion, *Py* pyrenoid, *SG* starch grain, *T* thylakoids, *V* vacuole, *VI* vacuolar inclusion. Scale bar = 1 µm (**a**, **c**, **d**) or 0.5 µm (**b**, **e**–**g**)

The *Lobosphaera* sp. in the studied cultures were characterized by accumulation of the carbon reserves in the form of cell inclusions such as starch grains (SG) and cytoplasmic lipid droplets (LD) (Figs. 3, 7, 8, SI3, SI4, Table 2). At the 9th day, the accumulation of SG in the vegetative cells of CC declined, whereas accumulation of LD increased as compared to the 2nd day of the experiment (Table 2). The cells of *Lobosphaera* sp. accumulated at the elevated P_i levels differed in size and number of their SG and LD which, in turn, depended on the P_i concentration in the medium. Notably, the C100 cells showed a declined SG accumulation as compared to the control. The opposite trend was recorded in the C25 and C50 cultures. After 2 days of incubation at the elevated P_i, the accumulation of LD increased 3 – 5 times as compared to CC. In the end of the experiment, the accumulation of LD decreased slightly in the C25 culture while in the C100 culture, the abundance of LD remained constant. The C50 culture showed the highest accumulation of SG and LD on the 9^{th} d of the experiment. In addition, the C25 and C50 culture possessed more plastoglobules in their chloroplasts than the control cells, whereas the C100 culture showed no difference in this regard.

Remarkably, manifestations of the osmotic stress, e.g., the gaps between the condensed cytoplasm and the cell walls

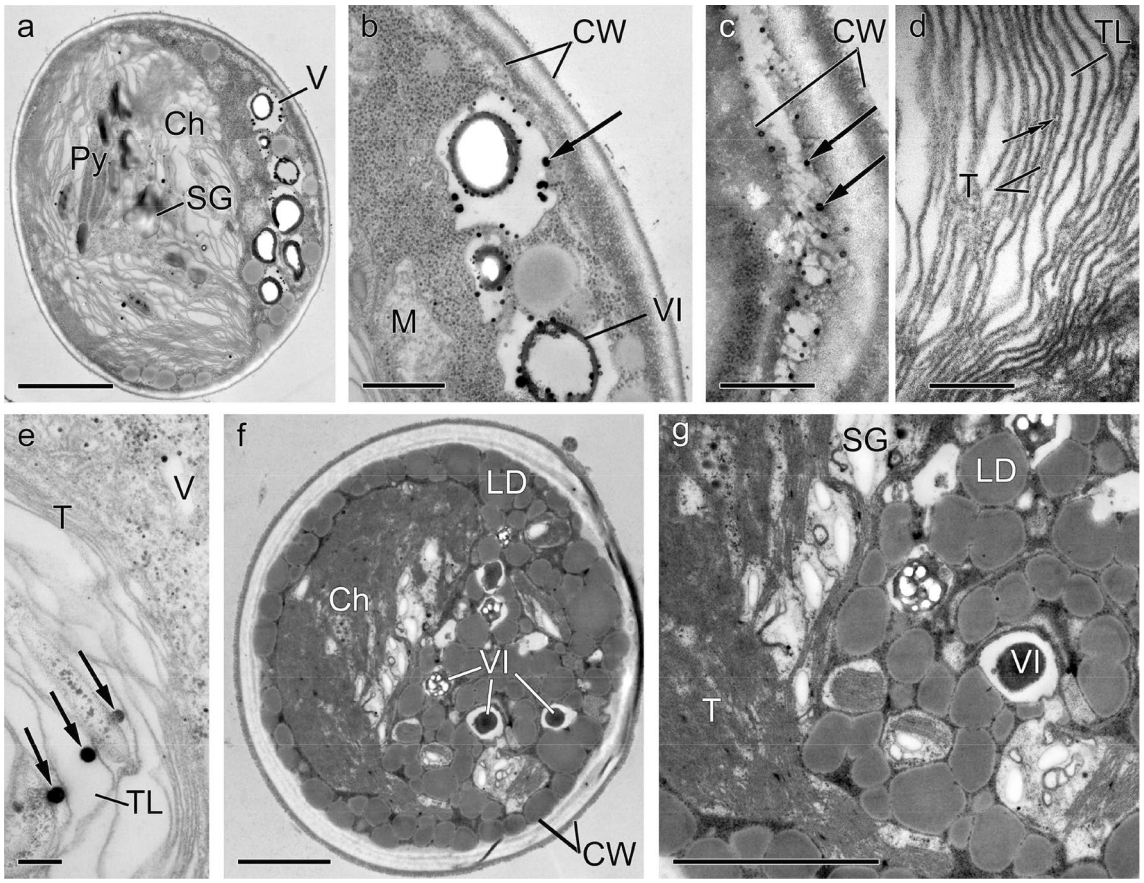

Fig. 8 Ultrastructure of the *Lobosphaera* sp. IPPAS C-2047 cells in C100 culture at 2th (**a**–**e**) and 9th (**f**, **g**) days of incubation. A survey image of the cells (**a**, **f**), vacuoles (**b**), chloroplasts (**d**, **e**, **f**), and cell wall (**c**); diverse electron opaque vacuolar inclusions (**a**, **b**, **f**, **g**), spherules in cytoplasm (**a**), cell wall (**c**), thylakoid lumen (**e**), and the destruction of photosynthetic apparatus (**f**, **g**). *Ch* chloroplast, *CW* cell wall, *LD* lipid droplet, *M* mitochondrion, *Py* pyrenoid, *SG* starch grain, *T* thylakoid, *TL* thylakoid lumen, *V* vacuole, *VI* vacuolar inclusion. Arrows indicate round-shaped electron opaque inclusions. Arrows with double tip indicate the local unstacking of thylakoids. Scale bars = 2 µm (**a**, **f**, **g**); 0.5 µm (**b**, **c**) and 0.2 µm (**d**, **e**)

Table 2 The accumulation of starch grains and lipid drops in *Lobosphaera* sp. IPPAS C-2047 vegetative cells incubated at elevated P_i levels

Experimental variant	Starch grains per section		Lipid drops per section	
	Incubation time			
	2 days	9 days	2 days	9 days
CC	20.9 ± 2.8[a]	16.4 ± 2.7	10.3 ± 3.0	23.6 ± 6.1
C25	30.8 ± 7.1	24.0 ± 2.9	33.2 ± 9.0	16.5 ± 3.3
C50	N/D[b]	32.0 ± 8.3	N/D	77.2 ± 14.5
C100	20.9 ± 6.4	4.3 ± 2.0	53.0 ± 15.8	55.6 ± 13.0

[a]Data are presented as means ± SE

[b]Not detected

(Fig. SI1a–c) and visually void mitochondria (Fig. SI1d) were noticed in *Lobosphaera* sp. incubated cultivated at the elevated P_i levels; they were especially pronounced in the C100 cells.

Already on the 2nd day of the experiment, the control cells of *Lobosphaera* sp. contained numerous vacuolar inclusions represented mostly by round-shaped granules of high electron density, 50–900 nm in size (T1 type, Table 3, Fig. 7a). The ring-like inclusions, 30–50 nm thick, occupying all the vacuole perimeter (T3 type, Table 3) and round-shaped inclusions of moderate electron density, 40–100 nm in diameter accompanied by small, scattered granules, 10–30 nm in size (T4 type, Table 3) were observed in a small part of cells.

Vacuole inclusions were enriched in P and O with the presence of N, Ca, and Mg (Fig. SI5a). We also noticed the round-shaped inclusions looking like electron-dense spherules 10 – 50 nm in size (T2 type, Table 3) rarely found in the cytoplasm or in the stroma of the chloroplasts.

On the 2nd d of the experiment, the vacuolar inclusions in C25, C50, and C100 cultures were represented mostly

Table 3 The effect of elevated external P_i concentrations on the diversity and abundance of the P-containing inclusions in *Lobosphaera* sp. C-2047 cells

Experimental variant	Inclusion type	Localization	Representative figure	Incubation time	
				2 days	9 days
CC	T1[1]	Vacuoles	Figure 7a	+++[f]	+++
	T2[2]	Cytoplasm, stroma of chloroplasts	–	+	+
	T3[3]	Vacuoles	–	+	+
	T4[4]	Vacuoles	–	+	++
	T5[5]	Cytoplasm	–	N/F[g]	N/F
C25, C50	T1	Vacuoles	Figures 7d, SI3e	+	+++
	T2	Most of the vegetative cell compartments; sporangia envelopes and inter-spore matrix	Figures 7c, d, SI3c, d, f, SI4b	+++	+++
	T3	Vacuoles	Figures 7 c, SI3a, d, SI4a	+++	+
	T4	Vacuoles	Figure 7c	++	+
	T5	Cytoplasm	–	+	+
C100	T1	Vacuoles	Figure 8g	N/F	+++
	T2	Most of the vegetative cell compartments; sporangia envelopes and inter-spore matrix	Figures 7e, 8a–c, e	+++	+++
	T3	Vacuoles	Figures 7e, 8a, b	+++	+
	T4	Vacuoles	–	N/F	N/F
	T5	Cytoplasm	Figure 7f	++	+++

[a]Round-shaped granules of high electron density, 150–900 nm in diameter

[b]Round-shaped inclusions of high electron density (spherules), 10–50 nm in diameter

[c]Ring-like structures of high or uneven election density, 30–50 nm thick

[d]Round-shaped inclusions of moderate electron density, 40–100 nm in diameter accompanied by small, scattered granules, 10–30 nm in size

[e]Small irregularly shaped particles of moderate electron density, 5–25 nm in size

[f]Abundance: scarce (+), moderate (++), ample (+++)

[g]Not found

by the ring-like inclusions of T3 type (Figs. 7c, e, f; 8a, b; SI3a, d; SI4a; Table 3), whereas T1 type inclusions, the most abundant in CC culture, were scarce or not identified. The T4 type inclusion appeared in C25, C50 culture (Fig. 7c), but was not found in C100 culture. The EDX spectra of T1, T3, and T4 types of vacuolar inclusions in cultures with high P_i resembled those in the CC culture and were attributed to PolyP (Figs. SI5a, c, e). The EDX spectra of the electron-transparent central part of the vacuoles were accompanied by the peaks of C, O, and Si but lacked the peaks of P and N (Fig. SI5d).

Numerous P-enriched inclusions of T2 type were detected in the cytoplasm (Figs. 7c, SI3d) as well as in the thylakoid lumen (Figs. 7d, 8e, SI3f, SI4b) and in the stroma of the chloroplasts (Figs. 7d, SI3b), in vacuoles (Figs. 7c, 8b), cell wall (Figs. 7e, 8c), mitochondria and the nuclei (Fig. 7f). These inclusions were much more abundant in the *Lobosphaera* sp. cells incubated at the elevated P_i levels as compared to control (Table 3). At high P_i T2 type inclusions were also found in the gaps under external cell wall layers (Fig. 7e), in the sporangia envelopes (Figs. SI3b, c) and in the spacer matrix separating the spores in zoo- and aplanosporangia (Fig. SI3d). In addition to that, small P-enriched irregularly shaped particles 5–25 nm in size were scattered in the cytoplasm (T5 type, Table 3, Figs. 7f). During 9 d experiment, the particles of T5 type were the amplest in the C100 culture, but these particles lacked in the control culture (Table 3). The EDX spectra of T5 inclusions contained the peaks of P, O, Ca, and Mg (Fig. SI5g) supporting their assignment to P-rich inclusions formed in assorted cell compartments during incubation at the elevated P_i levels. Importantly, the EDX spectra of the non-vacuolar inclusions both in control and in the elevated P_i-incubated cells did not contain the peak of N while all types of the vacuolar inclusions contained this peak (Fig. SI5).

After 9 days incubation at the elevated levels of P_i, T3 type inclusions in vacuoles considerably decreased, whereas the inclusions of T1 type dominated (Figs. 7g, 8f, SI3e, Table 3). The EDX spectra of T3 type inclusions in C25, C50, and C100 cultures resembled the spectra in CC, but the intensity of P peaks was considerably

higher (Fig. SI5h). Remarkably, numerous spherules and irregularly shaped particles were scattered over different compartments of *Lobosphaera* sp. apart from the vacuole resembling the picture documented on the 2nd day of the experiment.

4 Discussion

The investigated strain of *Lobosphaera* displayed an unusually high tolerance to the increased P_i concentrations in the medium. The *Lobosphaera* sp. cells retained viability in the presence of P_i amounts drastically (100 − 500 times) exceeding typical P_i concentrations in artificial growth media and environmental bioavailable P levels. We found that only extremely high P_i concentration of 100 g L^{-1} exerted a pronounced inhibitory effect on the *Lobosphaera*, whereas lower P_i concentrations (up to 50 g L^{-1}) caused only a mild stress. Arguably, this phenomenon has a complex nature involving a capability of storing of PolyP in the diverse cell compartments, acclimation of photosynthetic apparatus, as well as changes in the cell population structure and in its heterogeneity. The physiological and morphological peculiarities of the *Lobosphaera* sp. contributing, in our opinion, to its high P_i resilience are outlined below.

The changes in the condition of photosynthetic apparatus are very informative for estimation of stress responses in microalgae (see e.g., [31]) including *Lobosphaera* [32, 33]. Under our experimental conditions, up-regulation of NPQ accompanied the retention of photosynthetic activity by the cells incubated in the presence of the moderately elevated P_i levels (C25 and C50; Figs. 5a, 6). Interestingly, blocking the up-regulation of NPQ under the same conditions lead to a profound decline photosynthetic activity, but not at a low P_i concentration (Fig. 6). Our previous studies of *Lobosphaera* revealed participation of NPQ in acclimatory responses of this microalga to different stresses including nutrient starvation and chilling [32, 33]. Hence, its involvement is also likely under the high-phosphate stress conditions studied in this work,

Collectively, the physiological and ultrastructural studies suggest that the acclimation of *Lobosphaera* sp. to the high P_i levels completes, under our experimental conditions, within the first 2–3 days of exposure to the stressor. This is supported by steadily maintained photosynthetic activity at $P_i \leq 50$ g L^{-1}. A contrasting case of failed acclimation was represented by the cultures incubated with 100 g L^{-1} P_i. A pronounced decline of NPQ together with a drop of the photosynthetic activity (F_v/F_m) might manifest the exhaustion of the cell resources by the stress which turned to be too strong.

The studied P_i levels induced a sizeable decline of the biomass accumulation rate of *Lobosphaera* sp. but only slightly changed the composition of the major photosynthetic pigment groups: the increase in carotenoid-to-Chl ratio was below 10% of the value recorded in the control culture. The relative stability of the pigment ratio suggests that the acclimation of the cell to the high-P_i stress takes place mostly at the level of function, whereas the structural acclimation is less expressed. This hypothesis is supported by the ultrastructural evidence obtained: only the 100 g L^{-1} P_i provoked destructive changes in the assimilatory subcompartment of the cell (e.g., fragmentation of the thylakoids). By contrast, the cells incubated at the lower P_i levels (≤ 50 g L^{-1}) retained the overall functional integrity of the photosynthetic apparatus; at the same time, most of the studied cells possessed the more expanded thylakoid lumen as compared to the unstressed culture. This phenomenon might be related with the stress-induced increase in NPQ also documented in other microalgae species [34, 35] subjected to high irradiance or darkness, extreme temperatures, and abrupt changes in the medium composition [36, 37]. Mechanistically, the expansion of the lumen is believed to be a manifestation of the energization of the thylakoid membrane [38] during the build-up of NPQ, and facilitation of plastocyanin diffusion [23, 39, 40]. The contraction of the lumen following its expansion can be attributed to a decline in the cell capacity for light energy utilization and hence to its impaired ability to cope with the excess P_i stress, as obviously was the case in the cells incubated with 100 g L^{-1} P_i.

It is currently accepted that an increase in thermal dissipation of the absorbed light energy reduces the potential inhibitory effect and mitigates the risk of photooxidative damage [23]. This risk is high under stressful conditions disturbing the balance between the absorbed light energy and its utilization in the dark reactions of photosynthesis [31, 41, 42]. Such a reasoning was in line with the observed increase of carbon reserves in the cells apparent as an increase in LD and SG under the high-P_i stress. This ultrastructural response can be ascribed to the re-wiring of the cell metabolism in the stressed culture. Under the stress, the bulk of photosynthates is channeled into the biosynthesis of carbon-rich reserve compounds to re-establish the balance between the production and the consumption of the photosynthates [43–45]. This process can be augmented by the increased plastoglobuli formation harboring the lipids liberated in the processes of the controlled thylakoid dismantling. Overall, this process aims at adjusting of the light absorption cross-section of the cell [46]. Again, in the cells which failed to acclimate to the high P_i (9 days at 100 g L^{-1}), a significant reduction of SG was noticed indicative of the destruction of the assimilatory subcompartment and overall metabolic dysregulation of the cell.

Another spectacular phenomenon accompanying the acclimation of *Lobosphaera* sp. to high P_i was the delayed

formation of DAPI-stained vacuolar PolyP as compared to unstressed cells. It is known that the vacuolar compartment accommodates a considerable part of PolyP when P is ample in the surroundings of the microalgae cells [25]. This strategy allows to decrease the excess of P_i inside the cell and avoid the disturbance of metabolism, as the high levels of P_i can be toxic [47]. Under our experimental conditions, increased concentrations of P_i in the medium delayed the formation of the relatively large vacuolar PolyP inclusions observable under light microscope. At the same time, the results of EM with EDX demonstrated the abundance of vacuolar PolyP inclusions in *Lobosphaera* sp. at the initial stages of the high P_i exposure, but the morphology of the most diverse inclusions, described as thing ring-liked structures, differed from the large vacuolar inclusions in unstressed culture and probably did not allow to visualize them with DAPI-staining technique. In view of this finding, one can think that the vacuolar PolyP biosynthesis was somewhat impaired during the initial acclimation to the high P_i, but upon successful acclimation, it catches up with the amount of the P_i in the cells using the energy provided by photosynthetic apparatus. This suggestion was supported by our data on the dynamics of the vacuolar P-rich inclusions in *Lobosphaera* sp. (Table 3).

One should also mention an important role of PolyP in maintaining of the osmotic homeostasis of the microalgae cells [10]. This effect could be implemented through a specific polyphosphatase activity that hydrolyzes the long-chain PolyP to form ATP which is spent to support the cell homeostasis [10, 48]. Accordingly, the observed correlation between the delay of vacuolar PolyP visualization by DAPI and magnitude of high P_i stress probably indicates the participation of vacuolar PolyP in stress acclimation mechanism associated with PolyP hydrolysis.

Apart from changes in the vacuolar PolyP morphology in case of high-P_i stress, a vast increase in the abundance and diversity of small non-vacuolar P-containing inclusions was observed. In the cells incubated at the elevated P_i levels, such structures were found in every subcompartment of the cell. Taking into account the EDX results (Fig. SI5b, f, g), the peculiar morphology (Table 3), and the previously accumulated evidence [20], these inclusions represent the depot for the PolyP formed in the cell under the elevated P_i conditions. To the best of our knowledge, this is the first report on the structured PolyP inclusions in the thylakoid lumen of the chloroplast of the microalgae cell (Figs. 7d, 8e, SI3f), although the presence of amorphous P-containing matter in the thylakoids was documented previously [49]. The biosynthesis of long-chain PolyP in the form of broadly distributed non-vacuolar P-rich inclusions may reflect an emergency acclimation of the cell trying to convert the P_i excess to a less metabolically active form. This mechanism aims at control the formation of short-chain PolyP which can exert deleterious effects on the metabolism via protein misfolding and interfering in the matrix biosynthesis process [47].

Notably, the 100–500-fold increase of the external P_i exerted only 1.5–5.0 times increase of the internal P_i level. The moderate P accumulation seems to be crucial for the overall P_i tolerance of microalgae [3] including the studied *Lobosphaera* sp. and probably associated with the inhibition of the specific P_i uptake [50, 51] or the efflux of the excessive P_i [52].

Since large P_i concentrations were used in this work, the possible effects of the osmotic stress complementing the effects of P_i per se are very relevant. At the same time, we did not notice profound alterations in the average size of sporangia, young and mature cells cultivated under the excess P_i as compared to the unstressed culture (Fig. SI2). Moreover, only limited number of cells displayed the symptoms of plasmolysis in our experiments (Figs. 2, SI1), while most cells retained their structure and integrity. The obviously low influence of the osmotic stress can be attributed, at least in part, to the cell ability to limit the P_i uptake, the abundant synthesis of non-vacuolar long-chain PolyP enable to decrease the bioavailable P excess in cells, as well as the probable potential stabilizing effect exerted by hydrolysis of vacuolar PolyP.

Another determinant of the high P_i tolerance of *Lobosphaera* might be related to the stress response on the level of the cell population. In particular, the changes in the heterogeneity of cell population structure during stress might have a significant role in the operation of the stress-resilience mechanisms. The results of the microscopy revealed that zoosporangia were the most vulnerable to high P_i stress, they probably transformed into more P_i-tolerant aplanosporangia or eventually damaged. A similar response to unfavorable conditions was previously documented in *Trebouxia*, a relative of *Lobosphaera* sp., and explained by the better stress tolerance of aplanospores compared to zoospores lacking their own cell wall inside zoosporangia [53]. Interestingly, the 25 g L^{-1} P_i exerted the 5–8 time increase in aplanosporangia formation as compared to unstressed culture, whereas at the $P_i \geq 50$ g L^{-1} P_i, the level of aplanosporangia formation was low. The shift of the cell population toward aplanosporangia formation might be explained by a better protection of the cells inside sporangia from deleterious effects of a high external P_i. Probably, at $P_i \geq 50$ g L^{-1}, the formation of aplanosporangia was limited due to the lack of energy resources for cell reorganization or arrest of the sporogenesis. As a result, the domination of mature vegetative cells in the population structure was observed.

5 Conclusions

The remarkable P_i tolerance of the studied chlorophyte *Lobosphaera* sp. IPPAS C-2047 appears to be determined by several mechanisms. One of them is a versatile P-metabolism capable of rapid conversion of the exogenic P_i into metabolically safe PolyP stored in the many cell compartments in form of ample P-rich inclusions the acclimatory changes in the cell population structure and its heterogeneity. We also hypothesize that NPQ readily induced under the high-phosphate stress and the ultrastructure plasticity of the photosynthetic apparatus as well as the increase in the biosynthesis of carbon-rich reserve compounds could contribute to the observed resilience to the high external P_i. Last but not least, the cell ability to limit the P_i uptake and form ample vacuolar PolyP seems to play a role in retaining of the cell homeostasis under the high P_i stress in the *Lobosphaera* sp.

Supplementary Information The online version contains supplementary material available at https://doi.org/10.1007/s43630-022-00277-1.

Acknowledgements TEM studies were carried out at the Shared Research Facility "Electron microscopy in life sciences" at Moscow State University (Unique Equipment "Three-dimensional electron microscopy and spectroscopy"). Photosynthetic activity of microalgae was estimated using the Shared Research Facility "Phototrophic Organism Phenotyping." The support of the scientific and educational school of LMSU "Molecular technologies of living systems and synthetic biology" is appreciated.

Author contributions SV, EL, OG, and SA conceived and designed the experiments. SV, OG, OB, PS, OC, LS, and IS performed the experiments. SV, EL, GO, OB, AL, and AS analyzed the data. SV, AS, and GO wrote the manuscript with input from all authors. All authors reviewed and approved the final version of the manuscript.

Funding This work was funded by Russian Ministry of Science and Higher Education (Grant Number 075-15-2021-1396).

Data availability The datasets generated during and/or analyzed during the current study are available from the corresponding author on reasonable request.

Declarations

Conflict of interest The authors declare that they have no conflict of interest.

Ethical standards For this type of in vitro study, no ethical approval was required.

Consent to participate Not applicable.

Consent for publication Not applicable.

References

1. Brown, M. R., & Kornberg, A. (2004). Inorganic polyphosphate in the origin and survival of species. *Proceedings of the National Academy of Sciences, 101*(46), 16085–16087.
2. Solovchenko, A., Verschoor, A. M., Jablonowski, N. D., & Nedbal, L. (2016). Phosphorus from wastewater to crops: An alternative path involving microalgae. *Biotechnology advances, 34*(5), 550–564.
3. Cembella, A. D., Antia, N. J., & Harrison, P. J. (1984). The utilization of inorganic and organic phosphorus compounds as nutrients by eukaryotic microalgae: A multidisciplinary perspective: Part I. *Critical Reviews in Microbiology, 10*, 317–391.
4. Aitchison, P. A., & Butt, V. S. (1973). The relation between the synthesis of inorganic polyphosphate and phosphate uptake by *Chlorella vulgaris*. *Journal of Experimental Botany, 24*(3), 497–510. https://doi.org/10.1093/jxb/24.3.497
5. Solovchenko, A. E., Ismagulova, T. T., Lukyanov, A. A., Vasilieva, S. G., Konyukhov, I. V., Pogosyan, S. I., & Gorelova, O. A. (2019). Luxury phosphorus uptake in microalgae. *Journal of Applied Phycology, 31*(5), 2755–2770.
6. Kulaev, I. S., Vagabov, V., & Kulakovskaya, T. (2004). *The biochemistry of inorganic polyphosphates*. Wiley.
7. Li, F. J., & He, C. Y. (2014). Acidocalcisome is required for autophagy in *Trypanosoma brucei*. *Autophagy, 10*, 1978–1988.
8. Shi, X., Rao, N. N., & Kornberg, A. (2004). Inorganic polyphosphate in *Bacillus cereus*: Motility, biofilm formation, and sporulation. *Proceedings of the National Academy of Sciences, 101*(49), 17061–17065.
9. Rao, N. N., Gomez-Garcia, M. R., & Kornberg, A. (2009). Inorganic polyphosphate: Essential for growth and survival. *Annual Review of Biochemistry, 78*, 605–647.
10. Leitão, J. M., Lorenz, B., Bachinski, N., Wilhelm, C., Müller, W. E., & Schröder, H. C. (1995). Osmotic-stress-induced synthesis and degradation of inorganic polyphosphates in the alga *Phaeodactylum tricornutum*. *Marine Ecology Progress Series, 121*, 279–288.
11. Xie, L., & Jakob, U. (2019). Inorganic polyphosphate, a multifunctional polyanionic protein scaffold. *Journal of Biological Chemistry, 294*(6), 2180–2190.
12. Wang, Q., Wang, Z., Awasthi, M. K., Jiang, Y., Li, R., Ren, X., et al. (2016). Evaluation of medical stone amendment for the reduction of nitrogen loss and bioavailability of heavy metals during pig manure composting. *Bioresource Technology, 220*, 297–304.
13. Li, Q., Fu, L., Wang, Y., Zhou, D., & Rittmann, B. E. (2018). Excessive phosphorus caused inhibition and cell damage during heterotrophic growth of *Chlorella regularis*. *Bioresource Technology, 268*, 266–270.
14. Stanier, R. Y., Kunisawa, R., Mandel, M. C. B. G., & Cohen-Bazire, G. (1971). Purification and properties of unicellular blue-green algae (order Chroococcales). *Bacteriological reviews, 35*(2), 171–205.
15. Solovchenko, A., Merzlyak, M. N., Khozin-Goldberg, I., Cohen, Z., & Boussiba, S. (2010). Coordinated carotenoid and lipid syntheses induced in *Parietochloris incisa* (Chlorophyta, Trebouxiophyceae) mutant deficient in Δ5 desaturase by nitrogen starvation and high light. *Journal of Phycology, 46*(4), 763–772.
16. Ota, S., & Kawano, S. (2017). Extraction and molybdenum blue-based quantification of total phosphate and polyphosphate in *Parachlorella*. *Bio-protocol, 7*(17), e2539–e2539.
17. Strasser, R. J., Tsimilli-Michael, M., & Srivastava, A. (2004). Analysis of the chlorophyll a fluorescence transient. *Chlorophyll a fluorescence* (pp. 321–362). Dordrecht: Springer.

18. Colin, W. A., & Crofts, R. (1970). Energy-dependent quenching of chlorophyll *a* fluorescence in isolated chloroplasts. *European Journal of Biochemistry., 17*(2), 319–327.
19. Antal, T. K., Osipov, V., Matorin, D. N., & Rubin, A. B. (2011). Membrane potential is involved in regulation of photosynthetic reactions in the marine diatom *Thalassiosira weissflogii*. *Journal of Photochemistry and Photobiology B: Biology., 102*(2), 169–173.
20. Zharmukhamedov, S. K., & Allakhverdiev, S. I. (2021). Chemical inhibitors of photosystem II. *Russian Journal of Plant Physiology., 68*, 212–227.
21. Voronova, E. N., Volkova, E. V., Kazimirko, Y. V., Chivkunova, O. B., Merzlyak, M. N., Pogosyan, S. I., & Rubin, A. B. (2002). Response of the photosynthetic apparatus of the diatom *Thallassiosira weisflogii* to high irradiance light. *Russian Journal of Plant Physiology., 49*(3), 311–319.
22. Sun, K. M., Gao, C., Zhang, J., Tang, X., Wang, Z., Zhang, X., & Li, Y. (2020). Rapid formation of antheraxanthin and zeaxanthin in seconds in microalgae and its relation to non-photochemical quenching. *Photosynthesis Research., 144*, 317–326.
23. Ruban, A. V. (2016). Nonphotochemical chlorophyll fluorescence quenching: Mechanism and effectiveness in protecting plants from photodamage. *Plant Physiology, 170*(4), 1903–1916.
24. Gorelova, O. A., Baulina, O. I., Solovchenko, A. E., Chekanov, K. A., Chivkunova, O. B., Fedorenko, T. A., & Lobakova, E. S. (2015). Similarity and diversity of the *Desmodesmus* spp. Microalgae isolated from associations with White Sea invertebrates. *Protoplasma, 252*(2), 489–503.
25. Shebanova, A., Ismagulova, T., Solovchenko, A., Baulina, O., Lobakova, E., Ivanova, A., Moiseenko, A., Shaitan, K., Polshakov, V., Nedbal, L., & Gorelova, O. (2017). Versatility of the green microalga cell vacuole function as revealed by analytical transmission electron microscopy. *Protoplasma, 254*, 1323–1340.
26. Kokabi, K., Gorelova, O., Ismagulova, T., Itkin, M., Malitsky, S., Boussiba, S., Solovchenko, A., & Khozin-Goldberg, I. (2019). Metabolomic foundation for differential responses of lipid metabolism to nitrogen and phosphorus deprivation in an arachidonic acid producing green microalga. *Plant Science, 283*, 95–115.
27. Pouneva, I. (1997). Evaluation of algal culture viability and physiological state by fluorescent microscopic methods. *Bulgarian Journal of Plant Physiology, 23*(1–2), 67–76.
28. Kokabi, K., Gorelova, O., Zorin, B., Didi-Cohen, S., Itkin, M., Malitsky, S., et al. (2020). Lipidome remodeling and autophagic response in the arachidonic-acid-rich microalga *Lobosphaera incisa* under nitrogen and phosphorous deprivation. *Frontiers in Plant Science*. https://doi.org/10.3389/fpls.2020.614846
29. Merzlyak, M. N., Chivkunova, O. B., Gorelova, O. A., Reshetnikova, I. V., Solovchenko, A. E., Khozin-Goldberg, I., & Cohen, Z. (2007). Effect of nitrogen starvation on optical properties, pigments, and arachidonic acid content of the unicellular green alga *Parietochloris incisa* (Trebouxiophyceae, Chlorophyta). *Journal of Phycology, 43*(4), 833–843.
30. Watanabe, S., Hirabayashi, S., Boussiba, S., Cohen, Z., Vonshak, A., & Richmond, A. (1996). *Parietochloris incisa* comb. Nov. (Trebouxiophyceae, Chlorophyta). *Phycological Research, 44*(2), 107–108.
31. Jajoo, A. (2013). Changes in photosystem II in response to salt stress. *Ecophysiology and responses of plants under salt stress* (pp. 149–168). New York: Springer.
32. Zorin, B., Pal-Nath, D., Lukyanov, A., Smolskaya, S., Kolusheva, S., Didi-Cohen, S., Boussiba, S., Cohen, Z., Khozin-Goldberg, I., & Solovchenko, A. (2017). Arachidonic acid is important for efficient use of light by the microalga *Lobosphaera incisa* under chilling stress. *Biochimica et Biophysica Acta (BBA) Molecular and Cell Biology of Lipids, 1862*(9), 853–868.
33. Kugler, A., Zorin, B., Didi-Cohen, S., Sibiryak, M., Gorelova, O., Ismagulova, T., Kokabi, K., Kumari, P., Lukyanov, A., & Boussiba, S. (2019). Long-chain polyunsaturated fatty acids in the green microalga *Lobosphaera incisa* contribute to tolerance to abiotic stresses. *Plant and Cell Physiology., 60*(6), 1205–1223.
34. Solovchenko, A. E., Gorelova, O. A., Baulina, O. I., Selyakh, I. O., Semenova, L. R., Chivkunova, O. B., Scherbakov, P. N., & Lobakova, E. S. (2015). Physiological plasticity of symbiotic *Desmodesmus* (Chlorophyceae) isolated from taxonomically distant white sea invertebrates. *Russian Journal of Plant Physiology, 62*(5), 653–663.
35. Gorelova, O., Baulina, O., Ismagulova, T., Kokabi, K., Lobakova, E., Selyakh, I., et al. (2019). Stress-induced changes in the ultrastructure of the photosynthetic apparatus of green microalgae. *Protoplasma, 256*(1), 261–277.
36. Baulina, O. I. (2012). *Ultrastructural plasticity of cyanobacteria*. Springer Science & Business Media.
37. Topf, J., Gong, H., Timberg, R., Mets, L., & Ohad, I. (1992). Thylakoid membrane energization and swelling in photoinhibited *Chlamydomonas* cells is prevented in mutants unable to perform cyclic electron flow. *Photosynthesis research, 32*(1), 59–69.
38. Johnson, M. P., Brain, A. P., & Ruban, A. V. (2011). Changes in thylakoid membrane thickness associated with the reorganization of photosystem II light harvesting complexes during photoprotective energy dissipation. *Plant Signaling & Behavior, 6*(9), 1386–1390.
39. Johnson, M. P., Goral, T. K., Duffy, C. D., Brain, A. P., Mullineaux, C. W., & Ruban, A. V. (2011). Photoprotective energy dissipation involves the reorganization of photosystem II light-harvesting complexes in the grana membranes of spinach chloroplasts. *The Plant Cell, 23*(4), 1468–1479.
40. Pribil, M., Labs, M., & Leister, D. (2014). Structure and dynamics of thylakoids in land plants. *Journal of Experimental Botany, 65*(8), 1955–1972.
41. Bassi, R., & Dall'Osto, R. (2021). Dissipation of light energy absorbed in excess: The molecular mechanisms. *Annual Review of Plant Biology, 72*, 47–76.
42. Gollan, P. J., & Aro, E.-M. (2020). Photosynthetic signaling during high light stress and recovery: Targets and dynamics. *Philosophical Transactions of the Royal Society of London: Series B, Biological Sciences, 375*, 20190406. https://doi.org/10.1098/rstb.2019.0406
43. Domínguez, F., & Cejudo, F. J. (2021). Chloroplast dismantling in leaf senescence. *Journal of Experimental Botany, 72*(16), 5905–5918.
44. Kirchhoff, H. (2019). Chloroplast ultrastructure in plants. *New Phytologist, 223*(2), 565–574.
45. Bréhélin, C., & Kessler, F. (2008). The plastoglobuli: A bag full of lipid biochemistry tricks. *Photochemistry and Photobiology, 84*(6), 1388–1394.
46. van Wijk, K. J., & Kessler, F. (2017). Plastoglobuli: Plastid microcompartments with integrated functions in metabolism, plastid developmental transitions, and environmental adaptation. *Annual Review of Plant Biology, 68*, 253–289.
47. Gerasimaitė, R., Sharma, S., Desfougeres, Y., Schmidt, A., & Mayer, A. (2014). Coupled synthesis and translocation restrains polyphosphate to acidocalcisome-like vacuoles and prevents its toxicity. *Journal of Cell Science, 127*(23), 5093–5104.
48. Pick, U., Chitlaru, E., & Weiss, M. (1990). Polyphosphate-hydrolysis—A protective mechanism against alkaline stress? *FEBS letters, 274*(1–2), 15–18.
49. Voříšek, J., & Zachleder, V. (1984). Redistribution of phosphate deposits in the alga *Scenedesmus quadricauda* deprived of exogenous phosphate—An ultra-cytochemical study. *Protoplasma, 119*, 168–177.

50. John, E. H., & Flynn, K. J. (2000). Modelling phosphate transport and assimilation in microalgae; how much complexity is warranted? *Ecological Modelling, 125*(2–3), 145–157.
51. Hudek, L., Premachandra, D., Webster, W. A. J., & Bräu, L. (2016). Role of phosphate transport system component PstB1 in phosphate internalization by *Nostoc punctiforme*. *Applied and Environmental Microbiology, 82*(21), 6344–6356.
52. Jansson, M. (1993). Uptake, exchange and excretion of orthophosphate in phosphate-starved *Scenedesmus quadricauda* and *Pseudomonas* K7. *Limnology and Oceanography, 38*(6), 1162–1178.
53. Tschermak-Woess, E. (1989). Developmental studies in treboux-ioid algae and taxonomical consequences. *Plant Systematics and Evolution, 164*(1), 161–195.